



Structural Characterization of the J-domain of Tid1, a Mitochondrial Hsp40/DnaJ Protein

Dae-Won Sim^{1,‡}, Ku-Sung Jo^{1,‡}, Kyoung-Seok Ryu², Eun-Hee Kim², and Hyung-Sik Won^{1,*}

¹Department of Biotechnology, Konkuk University, Chungju, Chungbuk 380-701, Republic of Korea
²Division of Magnetic Resonance, Korea Basic Science Institute, Ochang, Chungbuk 363-883, Republic of Korea

(Received May 07, 2012; Revised May 29, 2012; Accepted June 08, 2012)

Abstract : Tid1, belonging to the Hsp40/DnaJ family of proteins, functions as a co-chaperone of cytosolic and mitochondrial Hsp70 proteins. In particular, the N-terminal J-domain of Tid1 (Tid1-JD) constitutes the major binding sites for protein-protein interactions with client proteins, including p53, as well as its partner chaperone, Hsp70. In the present study, soluble, recombinant protein of Tid1-JD could be obtained by using the pCold vector system, and backbone NMR assignments were completed using the isotope [¹³C/¹⁵N]-enriched protein. Far-UV CD result implied that Tid1-JD is an α -helical protein and the secondary structure determined using chemical shift data sets indentified four α -helices with a loop region containing the HPD (conserved tripeptide of His, Pro and Asp) motif. Additionally, NMR spectra under different conditions implied that the HPD motif, which is a critical region for protein-protein interactions of Tid1-JD, would possess dynamic properties.

Keywords: Tid1, mtHsp40, DnaJA3, J-domain, Secondary structure, HPD motif

INTRODUCTION

The specific pair of a heat shock protein 40 (Hsp40) and a heat shock protein 70 (Hsp70) is an essential chaperone system involved in protein translation, folding, unfolding, translocation, and degradation.^{1,2} In this machinery, Hsp70, which contains an ATPase domain and a substrate-binding

domain, provides the chaperone core, while Hsp40 functions as a co-chaperone that delivers substrate polypeptides to Hsp70 and stimulates the ATPase activity of Hsp70. In *E. coli*, the best studied Hsp70 is termed DnaK and its canonical partner Hsp40 is termed DnaJ.^{3,4} All types of Hsp40/DnaJ family proteins contain a so-called J-domain that is homologous to the N-terminal 73-residue domain of *E. coli* DnaJ.^{2,5} Basically, J-domain constitutes the major site for the binding of Hsp40 to Hsp70, thereby determining specificity of the Hsp40-Hsp70 interaction.^{1,6} In particular, the HPD motif (a highly conserved tripeptide of His, Pro and Asp) is an essential part of J-domain for its binding to the Hsp70 in the ATP state.^{4,6}

Human Tid1 (tumorous imaginal disc protein 1),⁷ also known as mtHsp40 (mitochondrial heat shock protein 40) or DnaJA3,^{2,8} is a unique member of Hsp40/DnaJ family that overwhelmingly localizes to the mitochondria.⁷⁻⁹ Although Tid1, with its N-terminal, mitochondrial targeting sequence, is efficiently translocated into the mitochondria, the protein plays many specific cellular functions including mitochondrial and nonmitochondrial activities, by interacting with cytosolic as well as mitochondrial Hsp70/DnaK proteins.⁸⁻¹¹ Some Hsp40 proteins function in client binding, as well as binding to their Hsp70 partners.¹ In addition, it has been suggested that the J-domain alone is sufficient for some cellular functions of certain Hsp40 proteins.^{1,6} In this respect, it would be reasonable to expect that the J-domain of Tid1 may drive functional specificity of the protein. Indeed, Tid1 has been recently identified as the protein that recruits the p53 tumor suppressor protein to the mitochondria, thereby initiating the mitochondrial apoptosis pathway.¹² Furthermore, the J-domain

has been suggested as the p53-binding site of Tid1.¹¹ Accordingly, the known interaction between p53 and the mitochondrial Hsp70 (also called mortalin)¹³ might be functionally regulated by Tid1, particularly through its J-domain. Detailed structural information on the J-domain of Tid1 (Tid1-JD) would contribute to the understanding of molecular mechanisms underlying functional diversity and specificity of the tumor-suppressive chaperone, Tid1. As an initial step of the structural study by NMR, production and preliminary structural characterization results of the recombinant Tid1-JD are reported in this paper.

EXPERIMENTAL

Cloning, Expression and Purification

In order to produce recombinant proteins of the J-domain, DNA fragments encoding the J-domain were PCR-amplified from the cDNA clones of Tid1, as a template, which were generously provided by Dr. S.-W. Kim (University of Calgary, Canada).^{11,12} The forward and reverse oligonucleotide primers were 5'- G GAA TTC **CAT ATG** TTG GCC AAA GAA GAT TAT TAT CA-3' and 5'-CCG CCG **CTC GAG** TCA AGA GCC GTA GGC ATC GTA C-3', respectively, where the *NdeI* and *XhoI* restriction enzyme cleavage sites are shown in bold. The PCR products were digested with *NdeI* and *XhoI* and then ligated into the *NdeI/XhoI*-digested expression vector

pColdI (Takara), to produce the ^{15}N -Tid1-JD with an N-terminal His₆-tag that facilitates protein purification. The constructed plasmid, verified via DNA sequencing, was transformed into the *E. coli* BL21(DE3)pLysS strain. The transformed cells were grown in M9 minimal medium at 37 °C. To prepare isotope-enriched proteins (^{15}N] and [$^{13}\text{C}/^{15}\text{N}$]Tid1-JD) for NMR, the M9 medium was supplemented with [^{13}C]glucose and/or [^{15}N]NH₄Cl as the sole source of carbon and nitrogen. When the A₆₀₀ of cell growth reached about 0.6, protein expression was induced at 15 °C by adding IPTG at a final concentration of 1 mM, and the induction was prolonged for 18 h. The harvested cells were then disrupted by sonication, and from the supernatant, the ^{15}N -Tid1-JD was purified via sequential chromatography on a nickel-affinity column (HisTrap FF, GE Healthcare) and a gel-filtration column (HiLoad 16/60 Superdex 75, Pharmacia). The tagged histidines were then cleaved with the protease, factor Xa, followed by the removal of factor Xa and other impurities via the sequential application of nickel-affinity and gel-permeation chromatography again. Finally, the purified solution was concentrated and buffer-exchanged by ultrafiltration (Amicon). Protein concentration was estimated via typical Bradford and BCA assays.

CD (Circular Dichroism) Spectroscopy

A standard far-UV CD spectrum of 25 μM Tid1-JD dissolved in a 20 mM Tris-HCl buffer (pH 7.0) containing 10 mM NaCl was measured at 20 °C on a Chirascan CD Spectrometer (Applied Photophysics, UK) equipped with a temperature-controlling unit, using a 0.5 mm path-length cell,

with a 1 nm bandwidth and a 1 nm step resolution. Three individual scans taken from 260 to 190 nm were summed and averaged, followed by the subtraction of the solvent CD signal. Finally, the CD intensity was normalized as the mean residue molar ellipticity (MRME).¹⁴

NMR Spectroscopy

NMR spectra were obtained on a Bruker Biospin Avance 800 spectrometer equipped with a cryoprobe, at KBSI (Korea Basic Science Institute). Conventional 2D-[¹H/¹⁵N]HSQC spectra were first measured with 0.3 mM of [¹⁵N]Tid1-JD dissolved in a 20 mM Tris-HCl buffer containing 300 mM NaCl, 1 mM dithiothreitol, and 7% D₂O, with varying pH and temperatures. Under the optimized condition finally decided, 3D HCCH-COSY and a series of triple resonance spectra, HNCACB, CBCA(CO)NH, HNCO and HN(CA)CO, were recorded on 0.9 mM of [¹³C/¹⁵N]Tid1-JD in the same buffer at pH 7.0, at 298 K. Sequential backbone NMR assignments for ¹⁵N^α, ¹³C^α, ¹³C^β, ¹³C^γ and ¹H^N atoms were performed by verifying and linking of peak clusters, according to the inter-residue ¹³C correlations.¹⁵ ¹H^α chemical shifts were also assigned, using the ¹³C^{α,β}-¹H^α correlations in the 3D HCCH-COSY spectrum. To determine the secondary structure, chemical shifts were directly referenced to DSS for the ¹H and indirectly for the ¹³C and ¹⁵N atoms, using the chemical shift ratio value suggested in the BMRB (<http://www.bmr.b.wisc.edu>), followed by the CSI (chemical shift index) and TALOS+ analysis on the ¹³C^α, ¹³C^β, ¹³C^γ and ¹H^α chemical shifts.¹⁶⁻¹⁸

RESULTS AND DISCUSSION

Our initial attempt to produce the soluble, recombinant Tid1-JD, using the overproducing pET vector systems, has failed since it resulted in insoluble inclusion bodies (data not shown). Finally, changing plasmids to pCold vectors, the subcloned Tid1-JD could be successfully over-expressed in soluble forms at low (15 °C) temperature (Figure 1A). The resulting construct, H6 Tid1-JD, contains 17 nonnative residues at the N-terminus, including the His₆-tag and the factor Xa cleavage site (underlined): MNHKVHHHHHHIEGRHM-. After cleavage of the tagged His₆-tag by the protease factor Xa, the resulting product, Tid1-JD, contains two nonnative residues, HM-, at the N-terminus.

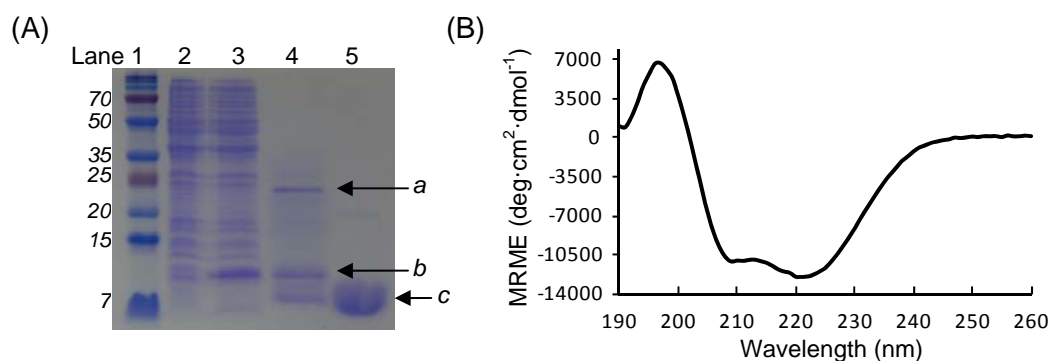


Figure 1. Expression, purification, and structural characterization of the recombinant Tid1-JD. (A) SDS-PAGE results: molecular size markers (lane 1, labeled in kDa), cell lysates before (lane 2) and after (lane 3) induction of the H6 Tid1-JD, cleavage of His₆-tag (lane 4), and the finally purified Tid1-JD (lane 5). Arrows indicate the positions of factor Xa (a), H6 Tid1-JD (b), and Tid1-JD (c). (B) Far-UV CD spectrum of the purified Tid1-JD.

We confirmed that the finally purified Tid1-JD behaves as a monomer in solution, by gel-filtration analysis (data not shown).^{15,19} The standard far-UV CD spectrum of Tid1-JD showed that the recombinant protein adopts a well-folded structure (Figure 1B), and the overall shape of the spectrum was characterized by a positive band at 196 nm and a strong negative band with double minima near 208 and 222 nm, which are indicative of a typical α -helical fold of a protein.

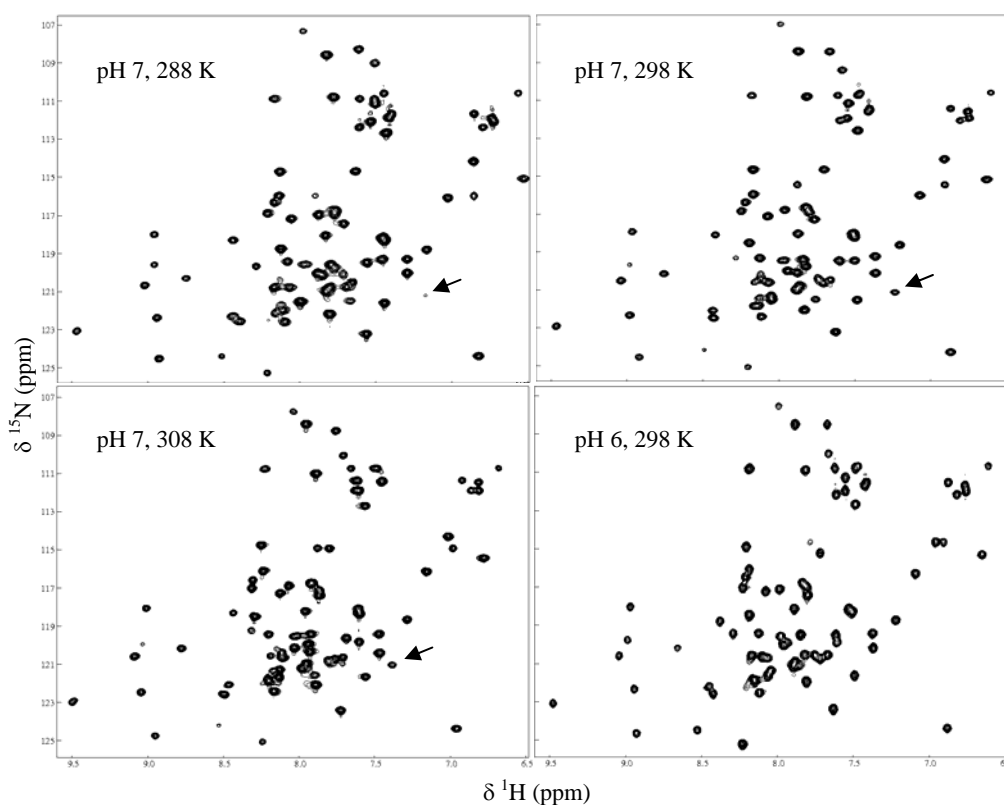


Figure 2. 2D- $[^1\text{H}/^{15}\text{N}]$ HSQC spectra Tid1-JD at different pH and different temperatures. The most variable peak in intensity depending on the condition is indicated by arrows.

Thus, in order to obtain more detailed structural information, NMR experiments were conducted. As the purified Tid1-JD at high concentrations readily aggregated at low ionic strength, leading to a time-dependent precipitation, solvent buffer for NMR contained a high (300 mM) concentration of NaCl salt. As shown in Figure 2, 2D- $[^1\text{H}/^{15}\text{N}]$ HSQC spectra of Tid1-JD showed a good dispersion of peaks and narrow line shapes, indicating again the well-folded conformation of the protein. In particular, spectral quality was the best at 298 K and pH 7.0, which condition was employed for 3D NMR experiments.

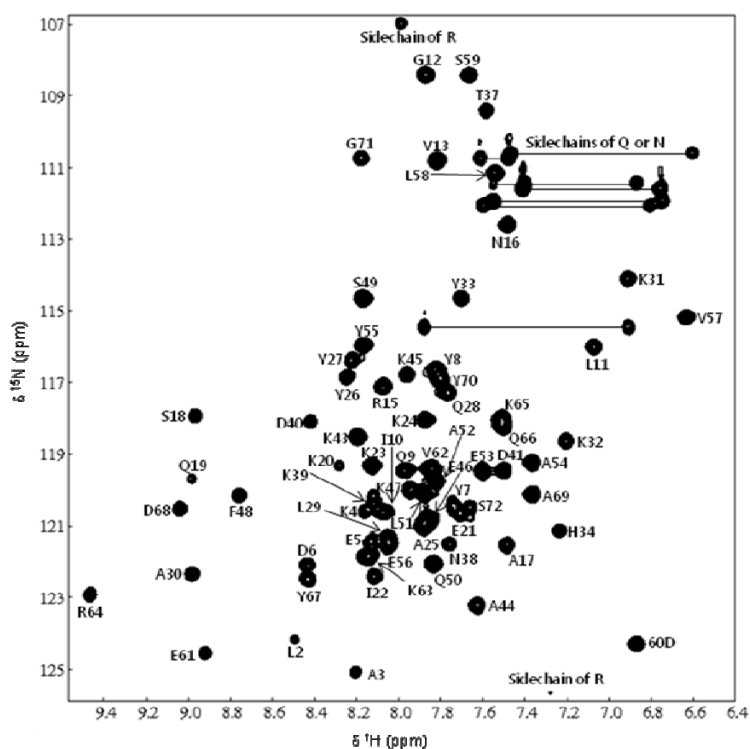


Figure 3. Sequence-specific assignments of Tid1-JD, labeled in the 2D- $[^1\text{H}/^{15}\text{N}]$ HSQC spectrum.

Figure 3 summarizes the sequence-specific backbone NMR assignments derived from the combined analysis of triple resonance spectra. Our recombinant Tid1-JD has 73 amino acids including three prolines, two arginines, two asparagines, five glutamines, and two non-native N-terminal residues, histidine and methionine. Both the two non-native residues didn't show amide proton signals in all NMR spectra, while the ^{13}C resonances of the second residue (Met) could be assigned, based on their correlation to the amide proton of the next residue (Leu), in the CBCA(CO)NH and HNCO spectra. Thus, we designated the non-native Met as the first residue in the numbering of amino acid sequence of the recombinant Tid1-JD (Figure 4). In the $[\text{}^1\text{H}/^{15}\text{N}]$ HSQC spectrum of Tid1-JD (Figure 3), sidechain NH signals from guanidino groups of the two arginines were detected as aliasing peaks and the seven pairs of NH_2 signals (indicated by lines in Figure 3) from sidechain amides of the seven glutamine and arginine residues could be also clearly distinguished from the backbone amide resonances. Finally, sequence-specific assignments of the remaining 68 (71 amino acids of native sequence minus three prolines) backbone amide proton and nitrogen resonances were obtained, except for the D36 residue, which didn't show the backbone amide signal in the $[\text{}^1\text{H}/^{15}\text{N}]$ HSQC spectra. Backbone $^{13}\text{C}^\alpha$, $^{13}\text{C}^\beta$, $^{13}\text{C}'$ and $^1\text{H}^\alpha$ resonances were also unambiguously assigned for the native sequence, including the D36 residue, based on intra- and inter-residue correlations in 3D spectra. Only the P35 residue could not be assigned, due to the absence of intra- and inter-residue correlations from amide protons.

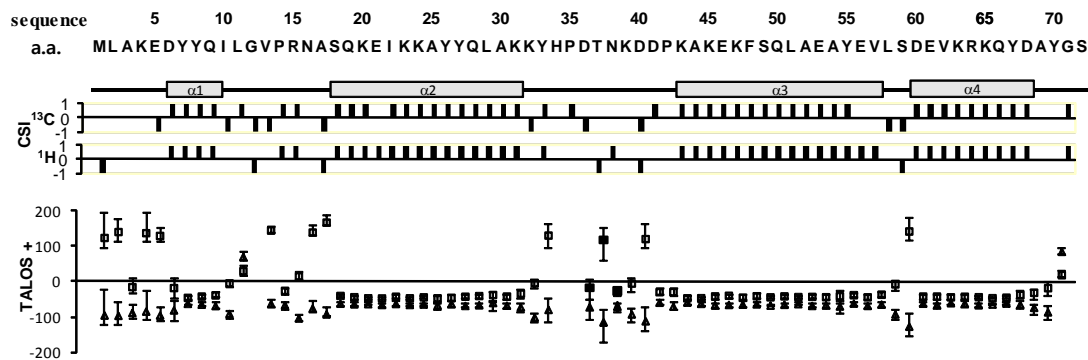


Figure 4. Secondary structure determination of Tid1-JD, using chemical shift data sets. The determined secondary structure elements are indicated by gray boxes for α -helices, along the amino acid sequence. In the CSI results, the mark “1” represents the α -helical tendency of the residue (downfield shifts of $^{13}\text{C}^{\alpha}$ or $^{13}\text{C}'$ resonances, and upfield shifts of $^{13}\text{C}^{\beta}$ or $^1\text{H}^{\alpha}$ resonances from their reference value ranges),^{16,17} while “-1” represents the opposite pattern (β -strand tendency). The chemical shift within the reference value range was marked as a “0”. ^{13}C CSI was finally summarized as a consensus-CSI derived by a simple “majority rule” (two or three out of three).²⁰ The length of error bars with the TALOS+-predicted backbone dihedral angles, ϕ (triangles) and φ (rectangles), indicate the standard deviation from the average.¹⁸

All of the assigned chemical shift data sets were applied to CSI and TALOS+ analysis to determine the secondary structure (Figure 4). The CSI and TALOS+ prediction results for secondary structure elements were in good agreement with each other. Finally, the determined secondary structure indicated that Tid1-JD is an α -helical protein, consistent with the CD result, and identified

four α -helix elements: $\alpha 1$ from D6 to Q9, $\alpha 2$ from S18 to K31, $\alpha 3$ from K43 to V57, and $\alpha 4$ from D60 to D68. Then, the conserved HPD motif (H34 to D36), being located within the loop region between $\alpha 2$ and $\alpha 3$, was adjacent to the $\alpha 2$. As mentioned above, the D36 residue didn't show amide proton signals under all conditions tested, probably due to chemical exchange or conformational equilibrium at an intermediate time scale. Similarly, the most variable peak in Figure 2 was finally assigned to the H34 residue, which was readily broadened or disappeared upon changing temperature or pH. The three internal residues, T37, N38 and K39, in addition to the N- and C-terminal residues, were classified as "Dyn" (dynamically disordered)¹⁸ in the TALOS+ prediction. All those results suggest exclusively dynamic properties of the inter-helix loop region between $\alpha 2$ and $\alpha 3$, including the HPD motif. Thus, it is postulated that the peculiar dynamics at the HPD motif could play a significant, functional role in its dynamic interaction with Hsp70 proteins.⁵

Taken all together, backbone NMR assignments of Tid1-JD were near completely achieved in this study and secondary structure was determined in solution. We expect that the present results will eventually provide the most fundamental and critical data for progressing studies of the fine 3D structure of Tid1 and its intermolecular interactions for diverse cellular functions.

Acknowledgment

This work was supported by the Korea Healthcare Technology R&D Project, Ministry for Health, Welfare & Family Affairs, Republic of Korea [A092006].

REFERENCES

1. H. H. Kampinga, E. A. Elizabeth, *Nat. Rev. Mol. Cell. Biol.* **11**, 579 (2010).
2. X. B. Qiu, Y. M. Shao, S. Miao, L. Wang, *Cell. Mol. Life. Sci.* **63**, 2560 (2006).
3. P. Genevaux, C. Georgopoulos, W.L. Kelley, *Mol. Microbiol.* **66**, 840 (2007).
4. A. Ahmad, A. Bhattacharya, R.A. McDonald, M. Cordes, B. Ellington, E.B. Bertelsen, E.R. Zuiderweg, *Proc. Natl. Acad. Sci. USA* **108**, 18966 (2011).
5. Li. Jingzhi, X. Quian, B. Sha, *Protein Pept. Lett.* **6**, 606 (2009).
6. F. Hennessy, W. S. Nicoll, R. Zimmermann, M. E. Cheetham, G. L. Blatch, *Protein Sci.* **14**, 1697 (2005).
7. J. Syken, T. De-Medina, K. Münger, *Proc. Natl. Acad. Sci. USA* **96**, 8499 (1999).
8. J. Proft, J. Faraji, J. C. Robbins, F. C. Zucchi, X. Zhao, G. A. Metz, J. E. Braun, *PLoS One* **6**, e26045 (2011).
9. B. Lu, N. Garrido, J. N. Spelbrink, C. K. Suzuki, *J. Biol. Chem.* **281**, 13150 (2006).
10. O. Iosefson, S. Sharon, P. Goloubinoff, A. Azem, *Cell. Stress Chaperones* **17**, 57 (2011).
11. L. N. Diane, A. N. Elwi, S.-W. Kim, *Oncotarget* **1**, 396 (2010).
12. B. Y. Ahn, D. L. Zajchowski, B. Lee, A. N. Elwi, S. -W. Kim, *Oncotarget* **29**, 1155 (2010).
13. O. Iosefson, A. Azem, *FEBS Lett.* **584**, 1080 (2010).
14. H. -S. Won, S. -H. Park, H. -E. Kim, H. -E. Kim, B. Hyun, M. Kim, B. -J. Lee, B. -J. Kim, *Eur. J. Biochem.* **269**, 4367 (2002).
15. D. -W. Sim, H. -C. Ahn, H. -S. Won, *J. Korean. Magn. Reson. Soc.* **13**, 108 (2009).
16. D. S. Wishart, B. D. Sykes, F. M. Richards, *Biochemistry* **31**, 1647 (1992).
17. D. S. Wishart, B. D. Sykes, *J. Biomol. NMR* **4**, 171 (1994).
18. Y. Shen, F. Delaqlio, G. Cornilescu, A. Bax, *J. Biomol. NMR* **44**, 213 (2009).
19. Y. -S. Lee, K. -S. Ryu, Y. Lee, S. Kim, K. -W. Lee, H. -S. Won, *J. Korean. Magn. Reson. Soc.* **15**, 137 (2011).
20. H. -S. Won, T. Yamazaki, T. -W. Lee, M. -K. Yoon, S. -H. Park, Y. Kyogoku, B. -J. Lee, *Biochemistry* **39**, 13953 (2000).